Spatio-temporal behaviors of a clock reaction in an open gel reactor

Khalid Benyaich, Thomas Erneux, Stéphane Métens, Sébastien Villain, and Pierre Borckmans

Citation: Chaos: An Interdisciplinary Journal of Nonlinear Science **16**, 037109 (2006); doi: 10.1063/1.2219703
View online: http://dx.doi.org/10.1063/1.2219703
View Table of Contents: http://scitation.aip.org/content/aip/journal/chaos/16/3?ver=pdfcov
Published by the AIP Publishing

Spatio-temporal behaviors of a clock reaction in an open gel reactor

Khalid Benyaich
Chimie Physique Nonlinéaire, CP 231, Université Libre de Bruxelles, Boulevard du Triomphe, B1050, Bruxelles, Belgium

Thomas Erneux
Optique Nonlinéaire Théorique, CP 231, Université Libre de Bruxelles, Boulevard du Triomphe, B1050, Bruxelles, Belgium

Stéphane Métens and Sébastien Villain[a)]
Matières et Systèmes Complexes, UMR CNRS 7057, Université Paris 7-Denis Diderot, 2 Place Jussieu, CC 7020, F75251, Paris Cedex 05, France

Pierre Borckmans[b)]
Chimie Physique Nonlinéaire, CP 231, Université Libre de Bruxelles, Boulevard du Triomphe, B1050, Bruxelles, Belgique

(Received 14 April 2006; accepted 13 June 2006; published online 27 September 2006)

The concentration profiles along the feeding direction of a one side fed gel reactor are analyzed for the iodate-arsenous acid reaction. Multiplicity of inhomogeneous stationary solutions is derived. It is also shown that such profiles may undergo oscillatory bifurcations under long range activation conditions. The bifurcation diagram is analyzed using a Galerkin approximation, the asymptotic validity of which is discussed. © *2006 American Institute of Physics*. [DOI: 10.1063/1.2219703]

Coexisting stable steady-state nonuniform concentration profiles have been observed experimentally for the same values of the parameters using an annular gel reactor continuously fed at one side by constant values of the chemical reactants.[1–3] Of particular physical interest is the observation that, when the diffusion coefficient of the autocatalyst becomes larger than that of the inhibitor, one of the profiles may undergo a time dependent bifurcation leading to oscillatory profiles.[4,5] This instability is a consequence of the nonuniform concentration profile of the steady state which results from the fixed boundary conditions. We examine this bifurcation problem by considering the iodate-arsenous acid (IAA) chemical reaction, a prototypic clock reaction.[6] The bifurcation diagram of the steady and time-periodic solutions is first examined numerically from the reaction-diffusion equations. Our results then motivate a one-mode Galerkin approximation of the reaction-diffusion equations. The resulting ordinary differential equations are studied in detail both analytically and numerically. They correctly predict the Hopf bifurcation instability and emphasize the role of key parameters. Finally, we discuss the asymptotic validity of the one-mode Galerkin approximation by exploring the conditions for a bifurcation from infinity (infinite width of the reactor).

I. INTRODUCTION

The so-called gel reactors have become a standard to study reaction-diffusion patterns resulting from chemical processes taking place in solutions. Since their first implementation they have undergone design modifications and presently the one-side fed reactor (OSFR) seems the most adequate to control the system in far from equilibrium conditions.[2] The core of the reactor consists of a piece of hydrogel, inert to the reactants and sheltering the reaction-diffusion patterns from any hydrodynamic disturbance. It is fed by diffusion through one of its faces with the reagents contained in a continuous stirred tank reactor (CSTR). The other faces are pressed against impermeable transparent walls. An advantage of such contraption is that it allows direct correlations between the reaction-diffusion dynamics in the gel and the chemical dynamics in the CSTR. The latter indeed gives valuable informations on the chemical kinetic processes taking place and, except for the geometry of the gel, provides all the controls of the OSFR through its feeding concentrations and residence time. Concentration variations in the gel are made visible with the aid of specific color indicators. In principle viewing is possible both along the feeding axis (axial direction) or orthogonally (transverse directions) to it. By construction the OSFR is an intrinsically *anisotropic* device. However, due to the typical size of the concentrations variations, the standard observation procedure only leads to information integrated across the thickness of the gel along the viewing direction. Furthermore, because of the experimental impediment (feeding capillaries, measurement electrodes, thermal jacket,…) both directions cannot be monitored simultaneously. Therefore such reactors presently arise in two different brands, the disk and annular reactors. Although the experimental discovery of Turing patterns stands as a landmark for the use of gel reactors,[7–9] the clear study of the much less glamorous phenomenon of spatial bistability, that was discovered in the chlorine dioxide-iodine (CDI) reaction with the aid of an annular OSFR,[1] is also of

[a)]Also at: Service de Chimie Physique Nonlinéaire, Université Libre de Bruxelles.
[b)]Electronic mail: Pborckm@ulb.ac.be

great importance. It emphasizes the fact that in the OSFR, the reaction-diffusion phenomena develop in a 3D world where axial profiles, due to the feeding, are always present. Therefore, 2D approximations that have been used to discuss the origin and competition between Turing and front (labyrinthine) patterns,[10] should always be assessed with care (this problem is discussed in Refs. 2 and 11). Spatial bistability is by no means a new phenomena. Indeed in their research to control reactors, the chemical engineers became aware, in the early 1960s,[12] that the coupling of chemical reactions and mass and/or heat diffusion transport phenomena in distributed parameter systems can cause the occurrence of multiple steady states. Aiming at predicting such multiplicities, criteria were then developed to determine sufficient conditions for the existence of a unique steady state.[13,14] Coincidently the mathematicians have also shown considerable interest for such nonlinear diffusion problems.[15] It has therefore showed up in numerous theoretical reaction-diffusion calculations giving rise to a huge literature, some related to our work (e.g., Refs. 16 and 17). The novelty resides with the annular OSFR that allows controlled experiments to be carried out. In this paper we re-examine the origin of spatial bistability, and discuss the time dependent oscillations that may emerge in long range activation conditions in the annular OSFR. Here we use the *p*H buffered iodate-arsenous acid clock reaction in a stoichiometric excess of arsenous acid. This system is endowed with an empirical rate law that has successfully been used to interpret a host of kinetic and reaction-diffusion phenomena in various other types of reactors: clock behavior and propagation of a conversion wave in a batch reactor,[18] morphological instability of such a wave,[19,20] existence of bistability between homogeneous steady states in a CSTR and characterization of various relaxational behaviors in the vicinity of the saddle-node bifurcations bracketing the bistability region.[21,22] Surprisingly the IAA reaction has never been run in an OSFR.

The plan of the paper is as follows: In Sec. II, we show that the bistability phenomenon is a consequence of the OSFR operating conditions by analyzing the reaction-diffusion equations in the case of equal diffusion coefficients. In Sec. III, we assume that the autocatalyst diffuses faster than the other reactant. We determine the bifurcation diagram numerically and find a branch of time-periodic standing waves. This bifurcation diagram is then analyzed using a one-mode Galerkin approximation. We find interesting conditions for the onset of these oscillations. Finally, we discuss the asymptotic validity of the Galerkin approximation by looking for small amplitude solutions.

II. SPATIAL BISTABILITY FOR THE IAA SYSTEM WITH EQUAL DIFFUSION COEFFICIENTS

As is well accepted the reaction-diffusion system describing the dynamics of the IAA system in the gel part of the OSFR is given by

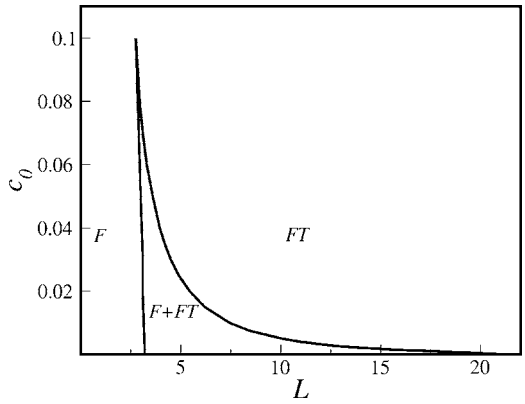

FIG. 1. Spatial bistability between the F and FT states occurs inside the cusped region in the (c_0, L) parameters plane; $d=d_{\exp}=0.0021$.

$$\partial_t X = f(X,Y) + D_X \partial_{xx} X,$$
$$\partial_t Y = -f(X,Y) + D_Y \partial_{xx} Y, \tag{1}$$

where $X=[\mathrm{I}^-]$ (autocatalyst), $Y=[\mathrm{IO}_3^-]$, and $f(X,Y)=(k_a+k_bX)XY$ (k_a and k_b are the kinetic constants, for which realistic values are given in the literature, multiplied by $[\mathrm{H}^+]^2$). In this paper we only discuss concentration profiles along the axial direction. Furthermore, we assume that the gel does not influence the dynamics of the CSTR. The complete set of equations describing the OSFR are given, for instance, in Refs. 1 and 2. The dynamics in the gel is then modelled with a Dirichlet boundary conditions at the CSTR-gel interface. A no flux boundary condition applies at the impermeable boundary.

If the diffusion coefficients are equal, the conservation law for iodine species imply $X+Y=X_0+Y_0=s_0=X_i+Y_i$, where X_0 and Y_0 are the concentrations inside the CSTR and X_i and Y_i those in the inflows of the CSTR. Using this relation leads to

$$\partial_t c = c(1-c)(c+d) + D\partial_{xx} c \tag{2}$$

with $c(x=0)=c_0$ and $\partial_x c|_{x=L}=0$. We have also defined $c=X/s_0$, $t'=t/\tau$, $x'=x/\sqrt{D\tau}$ with $d=k_a/k_b s_0$ and $\tau=1/k_b s_0^2$ and thereafter dropped the prime.

As shown by Fig. 2 of Ref. 21 the concentrations in the CSTR may take a continuous range of values by changing the CSTR control parameters (residence time and feed parameters). From now on, we shall assume that the concentration c_0 at the CSTR-gel boundary can take a continuous value from zero to one.

Our reaction-diffusion problem depends on three independent parameters. The feeding concentration c_0 of the gel and d that is an independent parameter function of the kinetic constants (hence temperature), the acidity of the solution, and the total quantity of iodine species present. The third parameter is the width L of the gel annulus. For sufficiently small d ($=d_{\exp}=0.0021$, if we use the parameters of Ref. 21) numerical integration shows that there exists a region of spatial bistability bounded by the cusp in the (c_0, L) plane (Fig. 1). For a typical value inside this region the two stable coexisting concentration profiles are shown in Fig. 2, together with their one-mode Galerkin approximation that we will

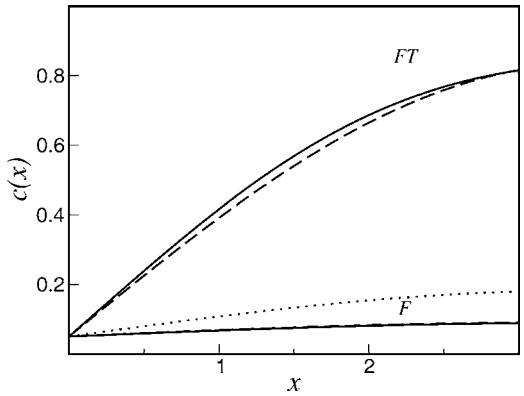

FIG. 2. Stable coexisting, F and FT, axial concentration profiles $c(x)$ in the gel part of the OSFR. The solid and dashed lines, respectively, correspond to the numerical integration of Eq. (1) and to its one-mode Galerkin approximation, that also allows us to draw the third unstable separatrix profile (dotted lines). $c_0=0.05$, $L=3.5$, $d=d_{\text{exp}}$.

later use. From Fig. 1 we note that, for small fixed c_0 and L, only one nearly flat profile may exist; the matter exchange between CSTR and gel is also small. Because small c_0 belongs to the flow branch of the CSTR, we name it the F profile. As L now increases, we enter the cusp and a second profile, called FT in Ref. 2 appears. As L is further increased only the FT profile remains. Because of the monotonous behavior of the concentration inside the gel, we may draw a standard bistability diagram (back-to-back saddle-node bifurcations) by plotting, for instance, the value of $c(L)$, the concentration at the impermeable boundary, as a function of L (Fig. 3). Similar cusps naturally also exists in the (d,L) and (c_0,d) planes, where the bistable region respectively widens toward the small d and c_0 values. However the FT numerical profile grows smoothly in contrast to the experimental ones in the CDI and chlorite-tetrathionate (CT) reactions.[1,5] This point is presumably related to the existence of only one chemical characteristic time in the model of the IAA system. Indeed the same feature is observed if the simplest kinetics scheme is used for the CT reaction.

We now explain the origin of spatial bistability using bifurcation theory.[11] If we define $w=c-c_0$ and $\xi=x/L$ ($\xi\in[0,1]$), Eq. (2) reads

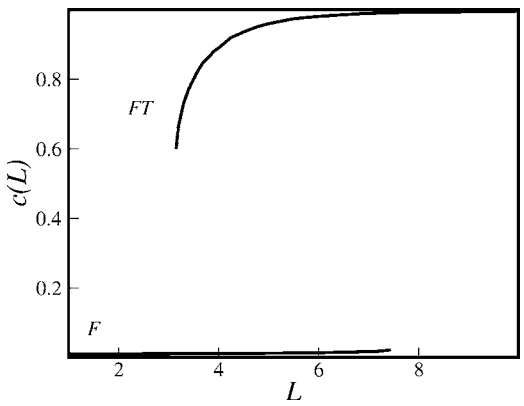

FIG. 3. Bistable bifurcation diagram for the concentration $c(L)$ at the impermeable boundary as a function of the size of the system in the axial direction. $c_0=0.05$, $d=d_{\text{exp}}$.

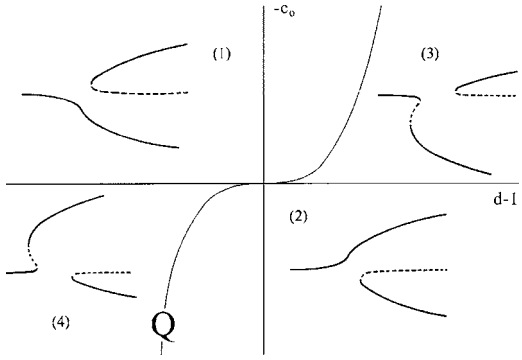

FIG. 4. Schematic bifurcation diagrams for $c_0\neq 0$ and $d\neq 1$. See discussion in the text. Adapted from Ref. 23.

$$\partial_t w = -\left[w^3 + (3c_0 - 1 + d)w^2 + (3c_0^2 + 2c_0(d-1) + d)w - c_0(1-c_0)(c_0+d)\right] + L^{-2}\partial_{\xi\xi} w \tag{3}$$

with $w(0)=\partial_\xi w(1)=0$.

If $c_0=0$ and $d=1$, the system of Eq. (3) is invariant for the $w\to -w$ (and also $c\to -c$) transformation. In this case $w=0$ is the only homogeneous steady state of the problem for any choice of L. Then the spectrum of the eigenvalues, $\Omega_n=L^2-n^2\pi^2/4$, of the Jacobian operator suggests that nontrivial solutions of the nonlinear problem may bifurcate from the point $(L,c_0,d)=(\pi/2,0,1)$. In order to calculate the solutions which bifurcate from this point, we introduce a small parameter η and expand w, L, d, and c_0 in power series of η:

$$w = 0 + \eta w_1(\xi,T) + \eta^2 w_2(\xi,T) + \eta^3 w_3(\xi,T) + \cdots,$$

$$L = \frac{\pi}{2}(1 + \eta L_1 + \eta^2 L_2 + \cdots),$$

$$d = 1 + \eta d_1 + \eta^2 d_2 + \cdots,$$

$$c_0 = 0 + \eta c_{01} + \eta^2 c_{02} + \eta^3 c_{03} + \cdots,$$

$$T = \eta^2 t + \cdots.$$

Substituting the preceding expansion into Eq. (3) and equating to zero the coefficients of successive powers of η, we find

$$c(x) = c_0 + A\,\sin(\pi x/2L) + O(\eta^2)$$

for the possible profiles, where A is the solution of the amplitude equation

$$\frac{3}{4}A^3 - \lambda A - \frac{4}{\pi}c_0 + \frac{8}{3\pi}(d-1)A^2 = 0 \tag{4}$$

with $\lambda=4L/\pi-\frac{3}{4}(d-1)^2+d-3$.

Equation (4) describes the unfolding of the pitchfork bifurcation, provided by the two first terms, hence when $c_0=0$ and $d=1$.

As we vary c_0 and d, various situations occur. The resulting bifurcation diagrams are conveniently given by representing the amplitude A as a function of λ. They are sketched as insets in Fig. 4. Let us now discuss the influence of the coefficients d and c_0 on the $c\to -c$ symmetry.

Keeping first $c_0=0$ and varying d, the pitchfork is transformed into a transcritical bifurcation. The saturation is then provided by a secondary saddle-node bifurcation. The sign of $(d-1)$ determines the direction of the $c\rightarrow -c$ symmetry breaking.

When $c_0\neq 0$, the complete unfolding appears as represented in Fig. 4. As c_0 plays the role of an imperfection parameter, we are left only with saddle-node bifurcations. The plane is divided into four regions by the two curves $c_0=0$ and $c_0=(32(1-d)/27\pi)^3$. The pitchfork case corresponds to the intersection of the two curves. As announced the typical bifurcation diagrams (A as a function of λ) are drawn in the four regions in the $(-c_0,d-1)$ plane. Since $d_{\exp}<1$ and $c_0>0$, the chemically valid region corresponds to the quadrant Q. As only branches corresponding to positive values of the concentrations are chemically relevant, the origin of spatial bistability lies in the crossing of the curve $c_0=(32(1-d)/27\pi)^3$ by varying c_0. This crossing corresponds to a critical point. The stability of the various branches may be determined by the slow time amplitude equation (not shown).

The physical mechanism of the spatial bistability can thus be apprehended through the study of the unfolding of the organizing pitchfork bifurcation. Mathematically, the simplest case of spatial bistability corresponds to the transcritical-saddle-node pair of bifurcation diagrams where one has the coexistence of the trivial $c(x)=0$, F profile, with an FT profile for the same boundary condition, $c_0=0$. This case is obviously experimentally unreachable since its corresponds to no input concentration in the gel, but will prove useful to simplify the determination of the possible bifurcations to time-periodic regimes.

III. SPATIAL OSCILLATIONS FOR THE IAA SYSTEM WITH LONG RANGE ACTIVATION

In the CT system where the autocatalyst, the proton, diffuses faster than the other species, the FT profiles may exhibit oscillatory behavior. We therefore wish to analyze this possibility in the IAA system when $\delta=D_Y/D_X<1$.

For conditions $d(=d_{\exp})$ lying inside the (c_0,L) cusp for $\delta=1$, we now lower the value of δ. Spatial bistability between the F and FT profile exists until $\delta=\delta_H$ (Fig. 5). At this point the FT profile undergoes a Hopf bifurcation and starts oscillating as a standing wave with the node at the feeding boundary, i.e., all the points along the profile oscillate in phase with an amplitude that increases as one moves away from the CSTR-gel boundary as shown in Fig. 6 for $u(L)$ and $u(L/2)$. We now have bistability between the stationary F profile and the oscillating FT profile. Further lowering the value of δ, the FT profile disappears through a saddle-loop bifurcation at $\delta=\delta_H^*$. The F state always remains stable but exhibits excitable properties in a neighborhood of $\delta<\delta_H^*$.[11] They will not be discussed here. Such sequence of behaviors has been observed in the CT reaction.[5]

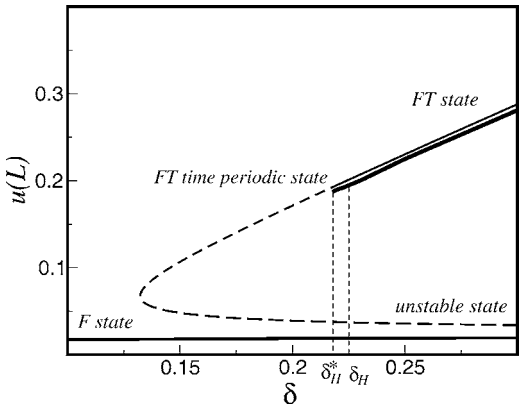

FIG. 5. Bifurcation diagram for $u(L)$ (reduced iodide concentration at the impermeable boundary represented by the full lines) as a function of δ the ratio of the diffusion coefficient of iodate and iodide. The FT state [larger values of $u(L)$] undergoes a Hopf bifurcation at δ_H, below which its amplitude oscillates as a standing wave with its node at $x=0$. The oscillating FT state is destroyed by another bifurcation at δ_H^*. To the left of that point, the system exhibits a region with excitable properties. The thin full and dashed lines are also the one-mode Galerkin approximation. $u_0=0.01$, $L=7.4$, $d=d_{\exp}$.

A. Bifurcation approach

We consider the two-variables IAA reaction-diffusion system supplemented by the boundary conditions $X=X_0$ and $Y=Y_0$ at $x=0$ and no flux conditions at $x=L$. Introducing dimensionless variables, we have

$$\begin{aligned}\partial_t F &= (F+u_0)(G+1)(F+u_0+d)+L^{-2}\partial_{\xi\xi}F,\\ \partial_t G &= -(F+u_0)(G+1)(F+u_0+d)+\delta L^{-2}\partial_{\xi\xi}G\end{aligned} \tag{5}$$

with $F(0)=G(0)=\partial_\xi F(1)=\partial_\xi G(1)=0$. We have defined $F=u-u_0$, $G=v-v_0$, and $\xi=x/L$ $(\xi\in[0,1])$, where $u=X/Y_0$, $v=Y/Y_0$, $t=t'/\tau$, and $x=x'/\sqrt{D_X\tau}$, $d=k_a/k_bY_0$, $\tau=1/k_bY_0^2$. Note that $v_0=1$ and $u_0=X_0/Y_0$.

We first consider the steady state problem for which we still have a conservation relation, namely $F+\delta G=0$. If $u_0=0$, Eq. (5) admits a uniform steady state $(F_s,G_s)=(0,1)$. Using this in Eq. (5), we are back with a single variable equation involving say F. Noticing further that for $d=\delta$ this

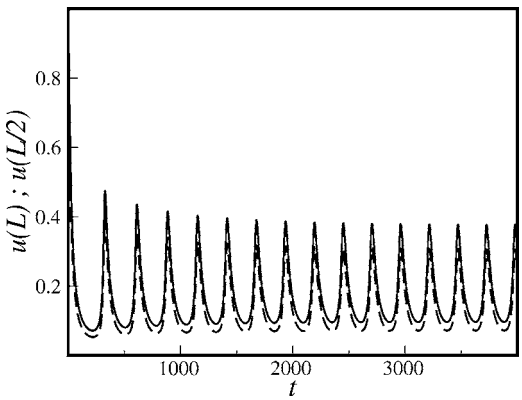

FIG. 6. Periodic time oscillations (after an initial transient) of the FT state measured at the impermeable boundary $[u(L)]$ and at midpoint in the system $[u(L/2)]$. The synchronism and amplitude difference are the prove of the standing wave character. $u_0=0.01$, $L=7.4$, $d=d_{\exp}$, $\delta=0.22$.

equation remains invariant with respect to the transformation $F \to -F$, we may again define an organizing center corresponding to a pitchfork bifurcation, $u_0=0$, $d=\delta$, and $L_c = \pi/2\sqrt{d}$. Indeed the linear instability conditions of this reference state, relating respectively to the determinant and trace of the Jacobian matrix read

$$L_n = n\pi/2\sqrt{d} < L_n' = n\pi\sqrt{(1+\delta)}/2\sqrt{d} \tag{6}$$

as δ is positive. So a steady state bifurcation always prevails, and occurs for $L_c=\pi/2\sqrt{d}$. No Hopf bifurcation can be anticipated at this point.

The emergence of spatial bistability in the two-variables model also occurs through the unfolding of a pitchfork bifurcation as previously discussed. The presence of δ does not bring any new stationary behavior and one finds the bifurcations diagrams discussed for the equal diffusion coefficients case by varying u_0 and $d-\delta$.

Now $F=A\sin(\pi\xi/2)+O(\eta^2)$ and $G=-(A/\delta)\sin(\pi\xi/2)+O(\eta^2)$, where the amplitude A satisfies

$$\frac{3}{8}A^3 + \frac{1}{8}\left(3d^2 - 10\delta d + \delta^2\left(15 - \frac{16}{\pi}L\sqrt{\delta}\right)\right)A - \frac{2}{\pi}\delta^2 u_0 - \frac{4A^2}{3\pi}(d-\delta) = 0.$$

Our bifurcation analysis, limited to the vicinity of the organizing center, does not predict the emergence of the time-periodic regimes observed numerically from the full original reaction-diffusion equations. In order to progress analytically, we shall examine a one-mode Galerkin approximation of the IAA reaction-diffusion equations. Our motivation comes from the previous observation that the numerical steady-state profiles were well approximated by a single sine function. From the reduced equations, we determine Hopf bifurcation points that provide clues on the physical mechanisms responsible for the oscillatory instabilities in the OSFR. We discuss the asymptotic validity of the Galerkin approximation at the end of the paper.

B. Galerkin approximation

Specifically, we concentrate on the u and v reaction-diffusion equations given by

$$\begin{aligned} \partial_t u &= uv(d+u) + L^{-2}\partial_{\xi\xi}u, \\ \partial_t v &= -uv(d+u) + \delta L^{-2}\partial_{\xi\xi}v, \\ u(0,t) &= u_0, \quad v(0,t) = 1, \quad u_\xi(1,t) = v_\xi(1,t) = 0. \end{aligned} \tag{7}$$

The sine functions form a natural basis and our numerical results indicate that a one-mode approximation is sufficient. Therefore we consider $u(\xi,t)=u_0+A(t)\sin(\pi\xi/2)$ and $v(\xi,t)=1+B(t)\sin(\pi\xi/2)$, where $A(t)$ and $B(t)$ are evaluated by the standard Galerkin procedure. This produces the set of ordinary differential equations

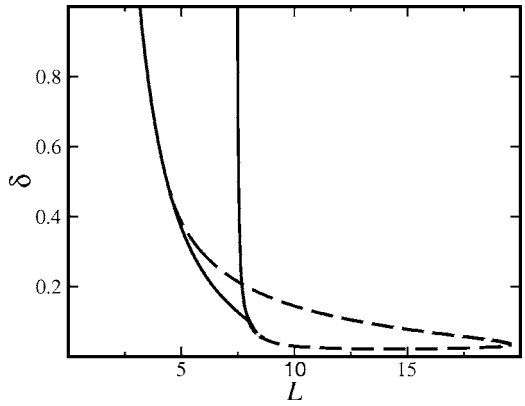

FIG. 7. X-shaped bifurcation diagram in the (δ,L) plane obtained from the one-mode Galerkin approximation. Plain lines are the loci of saddle-node bifurcations whereas the dotted lines are the loci of Hopf bifurcations. $u_0=0.01$, $d=d_{\exp}$.

$$\begin{aligned} d_t A &= g(A,B) - \pi^2 A/(4L^2), \\ d_t B &= -g(A,B) - \delta\pi^2 B/(4L^2), \end{aligned} \tag{8}$$

where

$$g(A,B) = c_3A^2B + c_2((d+2u_0)AB + A^2) + (2u_0+d)A + u_0(u_0+d)B + 3c_2u_0(u_0+d)/2$$

with $c_2=8/(3\pi)$ and $c_3=3/4$.

The steady state of Eqs. (8) determine the F and FT profiles for $u(x)$ and $v(x)$. The agreement with numerical integration of the full reaction-diffusion system [Eq. (7)] is of the same quality as that shown in Fig. 2 for the $\delta=1$ case. The method also allows the determination of the third unstable profile of the bistable (separatrix).

Using a symbolic solver, we may access to the full stability diagram, for instance in the (δ,L) plane (Fig. 7). It exhibits the general characteristics of a cross-shaped diagram,[24] that has also been analyzed for the CT system.[5] Whereas inside the cusp one has one Hopf bifurcation point leading to a spatial bistability diagram as shown in Fig. 8, outside the cusp another Hopf bifurcation may come into play on the FT profile.

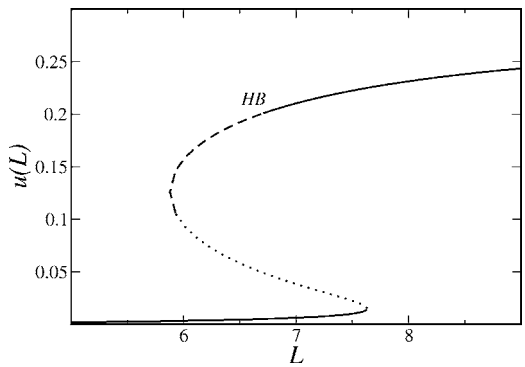

FIG. 8. Bistable bifurcation diagram, obtained through the one-mode Galerkin approximation, for the concentration $u(L)$ at the impermeable boundary as a function of the size of the system in the axial direction. The FT state undergoes a direct Hopf bifurcation at HB. The unstable stationary FT state is represented by dashed lines. $u_0=0.01$, $d=d_{\exp}$, $\delta=0.22$.

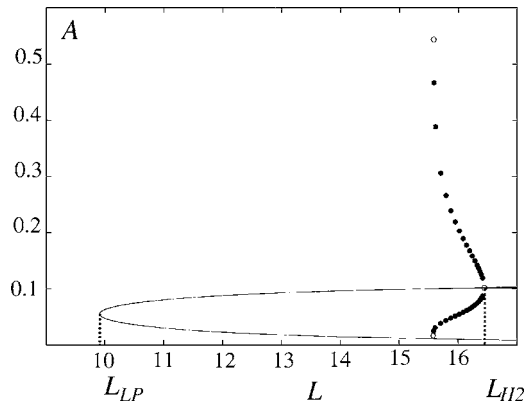

FIG. 9. Bifurcation diagram for the amplitudes of the *F* and *FT* states in the "perfect" $u(0)=0$ case, for $d=d_{\exp}$, $\delta=0.1$. L_{LP}, and L_{H2} are limit and Hopf bifurcation points, respectively. The transcritical bifurcation point ($L_c \simeq 34.278$) is off scale in order to be able to represent the envelope of the oscillations created by the Hopf bifurcation. These oscillations are destroyed by a saddle-node bifurcation.

C. Hopf scalings

To simplify the algebra, we narrow down our analysis to the "perfect case" ($u_0=0$) and extract scalings for the Hopf bifurcation points.

Now $g(A,B)=A[d+c_2(A+dB)+c_3AB]$. In addition to the trivial (*T*) steady state $A=B=0$, Eqs. (8) admit branches of nonzero steady states. In parametric form, $A=A(L^2)$ and $B=B(L^2)$ are given by

$$4L^2=\pi^2/(d+c_2A(1-d\delta^{-1})-c_3\delta^{-1}A^2)>0, \tag{9}$$

$$B=-\delta^{-1}A. \tag{10}$$

When $A=B=0$, we recover, from Eqs. (9) and (10) the previously found steady bifurcation point $L_c=\pi/(2\sqrt{d})$. Figure 9 shows the corresponding bifurcation diagram. The branches of nonzero steady states connect at the limit point $A=A_{LP}$. Using Eqs. (9) and (10) and the condition $dL^2/dA=0$, we get the saddle-node threshold L_{LP} and the corresponding amplitude A_{LP} as

$$A_{LP}=c_2(\delta-d)/(2c_3),$$

$$L_{LP}^2=\pi^2c_3(4c_3d+c_2^2\delta(1-d\delta^{-1})^2)^{-1}.$$

The characteristic equation for the growth rate Ω of the perturbations is

$$\Omega^2+\left[c_3A^2(\delta^{-1}+1)-c_2A(1-d)+\delta\frac{\pi^2}{4}L^{-2}\right]\Omega + \frac{\pi^2}{4L^2}[2c_3A-c_2(\delta-d)]A=0.$$

A Hopf bifurcation occurs if

$$c_3A^2\left(\frac{1}{\delta}+1\right)-c_2A(1-d)+\delta\frac{\pi^2}{4L^2}=0, \qquad [2c_3A-c_2(\delta-d)]A>0. \tag{11}$$

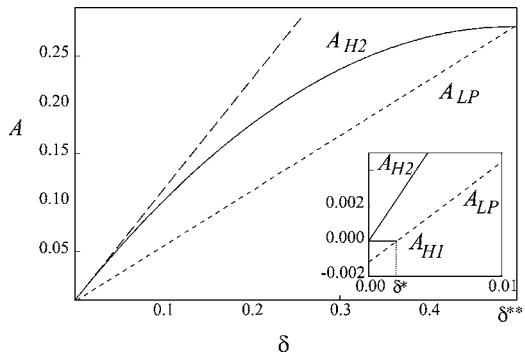

FIG. 10. Bifurcation lines for A_{LP} (small dashes), A_{H1} (full in inset), and A_{H2} (full in figure and inset), as a function of δ. The dashed line is the tangent at $\delta=0$ to A_{H2}. See discussion in the text; $d=d_{\exp}$.

Using Eqs. (9) and (10), we eliminate L^2 in Eq. (11) and obtain the following quadratic equation for A_H, the locus of Hopf bifurcations,

$$c_3A_H^2-c_2\delta A_H(1-\delta)+d\delta^2=0. \tag{12}$$

Moreover the inequality in condition (11) implies

$$A_H(A_H-A_{LP})>0. \tag{13}$$

For the chosen values of the parameters, the *FT* state undergoes a Hopf bifurcation at $L=L_{H2}$. Using Eq. (8) with $u_0=0$ we numerically determine the envelope of the oscillating branch of solution (see Fig. 9). In this case, the Hopf bifurcation is supercritical. Very close to the threshold L_{H2} the oscillations are harmonic but they rapidly become of relaxational type as we move away from L_{H2}. These oscillations die out through a saddle-loop bifurcation as their amplitude reaches the separatrix. There is thus a real correspondence between the results of the reaction-diffusion system and those of the Galerkin approximation.

Since Eq. (12) is a quadratic in A_H, the system may exhibit *two* Hopf bifurcations (cf. Fig. 10). We also note that the roots of Eq. (12) are always positive as $\delta<1$ (long range activation). Thus, the Hopf bifurcations *always* appear on the positive branch of the nontrivial states. In Fig. 10 we represent the loci of the various bifurcation points as a function of parameter δ. The Hopf bifurcation locus corresponds to a folium given by Eq. (12). Because of Eq. (13) and the fact that $A_H>0$, we need to be concerned only with the part that lies above A_{LP}, the saddle-node point.

Various behavior may now be distinguished as we lower δ from its value one. A Hopf bifurcation, A_{H2}, emerges from the saddle-node on the *FT* branch when δ becomes smaller than the abscissa of the upper A_H/A_{LP} intercept (δ^{**}). As δ continues to decrease, A_{LP} also decreases. Because $d(=d_{\exp})$ is small, the lower part of the folium only comes into play when $\delta<\delta^*$ (see inset Fig. 10), where another Hopf bifurcation A_{H1} emerges from the saddle-node. Further lowering δ, we reach $\delta=d$, where the transcritical and limit point bifurcations merge into a pitchfork. The two Hopf bifurcations A_{H1} and A_{H2} are still present on the positive *FT* branch [condition (13)] arising from the pitchfork bifurcation. Decreasing δ toward zero, the transcritical/saddle-node couple re-

emerges but now with $A_{LP}<0$, while the two Hopf bifurcations slide and collapse to $A_{H1}=A_{H2}=0$, as δ reaches zero.

Figure 10 reveals the importance of the small δ limit, where the two Hopf bifurcations coexist with progressively decreasing amplitudes A_H. Besides the effect of δ, the existence of two Hopf bifurcations result from a balance between quadratic and cubic nonlinearities. If c_3 were equal to zero only A_{H1} would exists. It is important to notice another fact. As δ approaches zero, assuming $d=O(\delta)$ and $A=O(\delta)$ (or smaller), Eq. (9) indicates that the values of L corresponding to both the Hopf and the saddle-node bifurcations move to infinity [i.e., $L=O(\delta^{-1/2})$]. The fact that, in this limit all critical Hopf amplitudes approach zero, suggests that a small amplitude time-periodic solution could be constructed in the singular large L limit. To further investigate this point, we determine the critical scaling laws for both Hopf bifurcation points as δ goes to zero, assuming $d=O(\delta)$. From Eq. (12), we find that A_{H1} and A_{H2}, respectively, scale like δ^2 and δ. Specifically, we obtain

$$A_{H1} = d\delta/c_2 + O(\delta^3) \text{ if } \delta < d \tag{14}$$

and

$$A_{H2} = c_2\delta/c_3 + O(\delta^2). \tag{15}$$

In the case of A_{H1}, we find from Eq. (10) that $B=O(\delta)$ and from the characteristic equation that the frequency of the oscillations at the Hopf point is $O(\delta^2)$. Together with $L^2=O(\delta^{-1})$, a singular perturbation analysis of a double zero eigenvalue is possible.[25–28] The analysis will be described in detail elsewhere. It shows that the one-mode Galerkin approximation is asymptotically valid in determining the leading behavior of the Hopf bifurcation point but not the Hopf bifurcation branch that requires us to take harmonic sine modes into account. In the case of A_{H2}, we find from Eq. (10) that $B=O(1)$. Because B is not proportional to δ, we cannot expect to capture the second Hopf bifurcation through the systematic construction of a small amplitude solution. In this case, we can only check the numerical validity of the one-mode Galerkin approximation by comparing the bifurcation diagrams of Eqs. (7) and (8).

IV. CONCLUSION

We have seen that the simple cubic type kinetics, best represented by the IAA reaction, still provides us with plenty of challenges.

In this work, we first showed that spatial bistability between stationary concentrations profiles, when all diffusion coefficients are equal, is the result of the boundary conditions imposed by the working conditions of the OSFR. It was explicitly carried out, with the help of bifurcation methods. However the main objective of the paper was to show that one of the nonuniform steady state regimes, appearing in such OFSR, is likely to exhibit a Hopf bifurcation, if the autocatalytic species diffuses faster than the other reactant. We demonstrate this by studying numerically the bifurcation diagram of the IAA reaction-diffusion system. We find that a branch of stable time-periodic standing waves may coexist with a stable steady state. It emerges from a Hopf bifurcation and terminates at a saddle-loop bifurcation. Our numerical bifurcation analysis is substantiated analytically by the study of a system of two amplitude equations obtained from a one-mode Galerkin approximation. We determine expressions for two possible Hopf bifurcation points and we emphasize the role of the different diffusion coefficients and the need for both quadratic and cubic nonlinearities. In order to generalize our conclusions to arbitrary reaction-diffusion systems, we need to examine the perturbation of a degenerate Hopf bifurcation point. We show that this is possible for one of the two Hopf bifurcation points if we consider the singular limit of infinite lengths. The detailed analysis is long and delicate and will be described in a future publication.

Extending our system to 2D by taking into account the transverse y direction orthogonal to the feeding axis, we also succeeded, again using the bifurcation approach of Sec. II, to solve the metastability problem between the F and FT profiles. To proceed we calculate the shape and velocity of the front connecting the F and FT profiles that are, respectively, maintained at $+\infty$ and $-\infty$ in the y direction.[11] This result might prove useful to study the hydrodynamical density fingering of chemical fronts of spatially extended bistable chemical systems in open Hele-Shaw cells.[29]

We have further been able to calculate the steady bistable nonuniform concentration profiles for a sphere of gel immersed in the CSTR. We have then used those results in a mechanically active gel and been able to produce a self-oscillation of the radius of the gel sphere.[30] The calculation was carried out in the framework of a multidiffusional approach and complements previous results obtained for the CT reaction using a different approach.[31]

ACKNOWLEDGMENTS

T. E. and P. B. were supported by the Fonds National de la Recherche Scientifique (Belgium).

[1] P. Blanchedeau, J. Boissonade, and P. De Kepper, Physica D **147**, 283 (2000).
[2] P. Borckmans, G. Dewel, A. De Wit, E. Dulos, J. Boissonade, F. Gauffre, and P. De Kepper, Int. J. Bifurcation Chaos Appl. Sci. Eng. **12**, 2307 (2002).
[3] J. Boissonade, P. De Kepper, F. Gauffre, and I. Szalai, Chaos **3**, 037110 (2006) (this issue).
[4] J. Boissonade, E. Dulos, F. Gauffre, M. N. Kuperman, and P. De Kepper, Faraday Discuss. **120**, 253 (2001).
[5] M. Fuentes, M. N. Kuperman, J. Boissonade, E. Dulos, F. Gauffre, and P. Kepper, Phys. Rev. E **66**, 056205 (2002).
[6] I. R. Epstein and J. A. Pojman, *An Introduction to Nonlinear Chemical Dynamics* (Oxford University Press, Oxford, 1998).
[7] V. Castets, E. Dulos, J. Boissonade, and P. De Kepper, Phys. Rev. Lett. **64**, 2953 (1990).
[8] Q. Ouyang and H. Swinney, Nature (London) **352**, 610 (1991).
[9] B. Rudovics, E. Barillot, P. W. Davies, E. Dulos, J. Boissonade, and P. De Kepper, J. Phys. Chem. A **103**, 1790 (1999).
[10] K. J. Lee, W. D. McCormick, Q. Ouyang, and H. L. Swinney, Science **261**, 192 (1993).
[11] K. Benyaich, Ph.D. thesis, Université Libre de Bruxelles (2005).
[12] P. B. Weisz and J. S. Hicks, Chem. Eng. Sci. **17**, 265 (1962).
[13] R. Aris, Chem. Eng. Sci. **24**, 149 (1969).
[14] D. Luss in *Spatial Inhomogeneities and Transient Behaviour in Chemical Kinetics*, edited by P. Gray, G. Nicolis, F. Baras, P. Borckmans, S. Scott (Manchester University Press, Manchester, 1989), p. 103, and references therein.

[15]J. Shi, Ph.D. thesis, Brigham Young University (2003).
[16]P. Gray and S. Scott, *Chemical Oscillations and Instabilities* (Oxford University Press, Oxford, 1990).
[17]R. Lefever, M. Herschkowitz-Kaufman, and J. W. Turner, Phys. Lett. **60A**, 389 (1977).
[18]A. Saul and K. Showalter in *Oscillating and Traveling Waves in Chemical Systems*, edited by R. J. Field and M. Burger (Wiley, New York, 1985), p. 419.
[19]D. Horvath, V. Petrov, S. K. Scott, and K. Showalter, J. Chem. Phys. **98**, 6332 (1993).
[20]D. Horvath and K. Showalter, J. Chem. Phys. **102**, 2471 (1995).
[21]N. Ganapathisubramanian and K. Showalter, J. Chem. Phys. **84**, 5427 (1983).
[22]G. Dewel, P. Borckmans, and D. Walgraef, J. Phys. Chem. **88**, 5442 (1984).
[23]M. Golubitsky and D. G. Shaeffer, *Singularites and Groups in Bifurcations Theory* (Springer Verlag, Berlin, 1985).
[24]J. Boissonade and P. De Kepper, J. Phys. Chem. **84**, 501 (1980).
[25]J. P. Keener, Chem. Phys. **18**, 126 (1981).
[26]J. P. Keener, SIAM J. Appl. Math. **41**, 127 (1981).
[27]M. Baer and T. Erneux, SIAM J. Appl. Math. **46**, 721 (1986); **52**, 1651 (1992).
[28]P. A. Braza and T. Erneux, Phys. Rev. A **40**, 2539 (1989).
[29]A. De Wit, P. De Kepper, K. Benyaich, G. Dewel, and P. Borckmans, Chem. Eng. Sci. **58**, 4823 (2003).
[30]S. Villain, S. Métens, and P. Borckmans, J. Mech. Behav. Mater. (to be published).
[31]J. Boissonade, Phys. Rev. Lett. **90**, 188302 (2003); Chaos **15**, 023703 (2005).